

Conductance through geometrically frustrated itinerant electronic systems

A. A. Lopes,¹ B. A. Z. António,² and R. G. Dias²

¹*Institute of Physics, University of Freiburg, Hermann-Herder-Straße 3, 79104 Freiburg, Germany.*

²*Department of Physics, I3N, University of Aveiro,
Campus de Santiago, Portugal*

(Dated: July 8, 2014)

We study a two terminal electronic conductance through an AB_2 ring which is an example of the family of itinerant geometrically frustrated electronic systems. These systems are characterized by the existence of localized states with nodes in the probability density. We show that such states lead to distinct features in the conductance. For zero magnetic flux, the localized states act as a filter of the zero frequency conductance peak, if the contact sites have hopping probability to sites which are not nodes of the localized states. For finite flux, and in a chosen orthonormal basis, the localized states have extensions ranging from two unit cells to the complete ring, except for very particular values of magnetic flux. The conductance exhibits a zero frequency peak with a dip which is a distinct fingerprint of the variable extension of these localized states.

PACS numbers: 73.23.-b, 81.07.Nb

I. INTRODUCTION

The conductance through molecular devices, nanowires and other nano systems has been extensively studied both theoretically and experimentally. Nano transport phenomena such as Coulomb blockade¹, conductance quantization², resonant tunneling³, quantum interference, Aharonov-Bohm oscillations in the conductance^{4,5} are now well understood.

The conductance fingerprints of localized states, however, induced by the topology of a nanocluster^{6–26} has never been addressed as far as we know. Do these localized states inhibit the electronic transport through the cluster or is the conductance indifferent to their existence? The answer is rather complex and unexpected. In this paper we show that, in the case of the AB_2 ring (which is an example of the family of itinerant geometrically frustrated electronic systems^{6–26}), these localized states act as zero frequency conductance absorbers for zero magnetic flux, but surprisingly generate a dipped zero frequency conductance peak when magnetic flux is applied. Similar features should be observed in the conductance through other elements of the family of the itinerant geometrically frustrated electronic systems of the Lieb lattice kind, that is, systems which display localized states with nodes in their probability density²⁷.

This paper is organized in the following way: First we recall recent exact results about the eigenstates of the AB_2 tight-binding ring, and in particular we discuss the form of the localized states when magnetic flux is present. Next we discuss the conductance through an AB_2 ring for several different scenarios including different placements of the conducting leads and different values of the threading flux.

II. EXACT DIAGONALIZATION OF THE AB_2 CHAIN AND LOCALIZED STATES

In order to address the phenomena of coherent transport through an AB_2 ring, we consider a two terminal set up of one-dimensional (1D) tight-binding leads coupled to the AB_2 ring, as depicted in Fig. 1. Our results are easily generalized to the case of 3D leads as long as only one site of each lead contacts the cluster. We shall often focus on the case where the number of cells of the AB_2 ring, N_c , is equal to 4, and assume that each plaquette is threaded by an identical magnetic flux, ϕ .

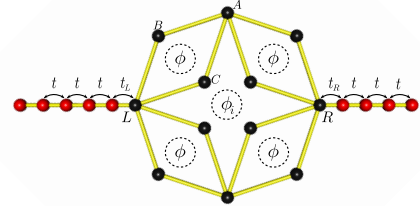


FIG. 1: The AB_2 ring is connected at sites L and R , to semi-infinite tight binding leads via a hopping amplitude t' . Except where otherwise stated, the hopping amplitude of the leads is taken to be the same to that of the star, t . Here it is shown the situation for $N_c = 4$, a particular case we will study in detail. The magnetic fluxes threading the plaquettes and the inner ring are respectively ϕ and ϕ_i .

A. Exact diagonalization

The Hamiltonian of the full system is given by

$$H_{\text{ring}} + H_{\text{leads}} + H_{\text{LR}}, \quad (1)$$

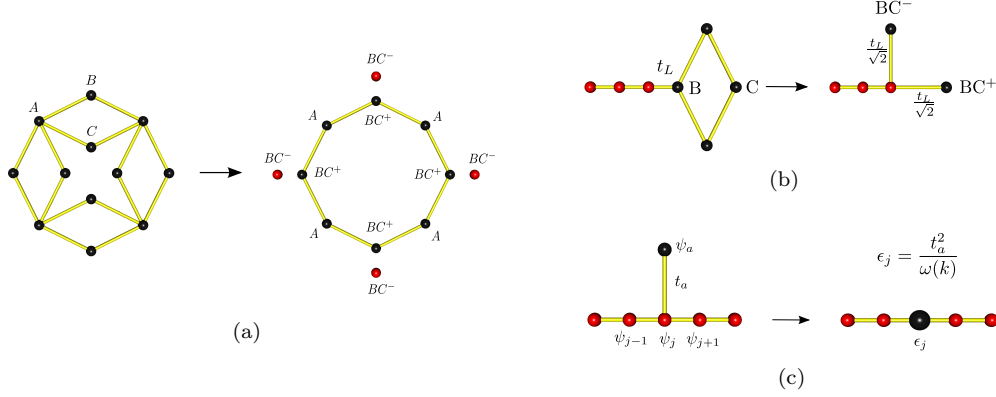


FIG. 2: (a) In the absence of magnetic flux, rewriting the Hamiltonian in the basis of antibonding BC^- , bonding BC^+ and A states, one obtains a tight-binding ring of sites A and bonding BC sites (with hopping constant $\sqrt{2}t$) and a ring of decoupled anti-bonding BC states. (b) The hopping term from the left lead to a B site of the AB₂ ring, in the basis of antibonding BC, bonding BC and A states, becomes $t_L/\sqrt{2}$. (c) For a incident particle with energy $\omega = -2t \cos(k)$, an extra transverse hopping t_a to a dangling site effectively modifies the on-site energy of site j to $\epsilon_j = t_a^2/\omega$.

where H_{leads} is the Hamiltonian of the isolated leads, assumed to be semi-infinite,

$$H_{\text{leads}} = -t \sum_{j=1}^{\infty} \sum_{\sigma=\uparrow,\downarrow} |a_{j,\sigma}\rangle \langle a_{j+1,\sigma}| + |a_{-j-1,\sigma}\rangle \langle a_{-j,\sigma}| + \text{H.c.}, \quad (2)$$

where $|a_{j,\sigma}\rangle$ is a lead Wannier state at site j and with spin σ . $j \in (-\infty, -1]$ correspond to left lead states while $j \in [1, \infty)$ correspond to right lead states. H_{star} is the Hamiltonian for an AB₂ chain with N_c unit cells,

$$H_{\text{ring}} = -t \sum_{j=1}^{N_c} \sum_{\sigma=\uparrow,\downarrow} e^{i\phi_o/2N_c} (|A_{j,\sigma}\rangle \langle B_{j,\sigma}| + |B_{j,\sigma}\rangle \langle A_{j+1,\sigma}|) + e^{-i\phi_i/2N_c} (|C_{j,\sigma}\rangle \langle A_{j,\sigma}| + |A_{j+1,\sigma}\rangle \langle C_{j,\sigma}|) + \text{H.c.},$$

where $|A_{j,\sigma}\rangle$, $|B_{j,\sigma}\rangle$, $|C_{j,\sigma}\rangle$ correspond to states on A, B and C sites, respectively, of the j th cell/plaquette, with spin σ . Here we have chosen a gauge such that the Peierls phases are equally distributed in the inner ring and in the outer ring. In Fig. 1, an AB₂ ring is shown with a magnetic flux ϕ threading each plaquette and a magnetic flux ϕ_i threading the inner ring. The magnetic flux enclosed by the outer ring is $\phi_o = \phi_i + 4N_c\phi/4$ and we introduce an auxiliary flux ϕ' such that $\phi_o = \phi' + 2N_c\phi/4$, $\phi_i = \phi' - 2N_c\phi/4$. The inner sites in the AB₂ ring of Fig. 1 are denoted as C sites and the outer sites as B sites. Spinal sites are denoted as A sites. The hybridization between the AB₂ ring and the leads is given by

$$H_{\text{LR}} = - \sum_{\sigma=\uparrow,\downarrow} t_L |a_{-1,\sigma}\rangle \langle X_{L,\sigma}| + t_R |a_{1,\sigma}\rangle \langle X_{R,\sigma}| + \text{H.c.}, \quad (3)$$

where $t_{L,R}$ are the hopping amplitudes coupling the leads and the star and X stands for an A, B or C site depending on where the left (L) and right (R) contacts are. Since

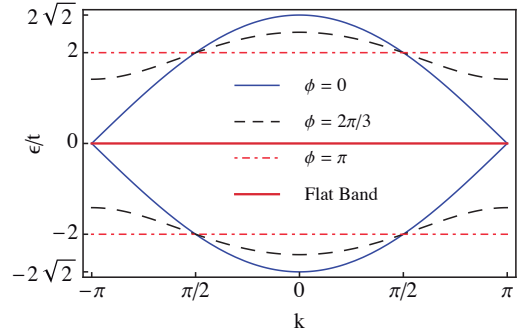


FIG. 3: Dispersion relation of the AB₂ ring for $\phi' = 0$ and several values of ϕ . Note that a gap opens between the localized band and the itinerant bands when there is a finite flux. Also, for $\phi = \pi$ all bands are flat, and therefore, all states are localized.

we don't consider spin-spin interactions, each spin channel is independent and we disregard spin in the rest of the paper, without any loss of generality.

Without interactions, the tight-binding AB₂ chain has a flat band even in the presence of magnetic flux (Fig. 3 displays the dispersion relation of the nearest neighbor AB₂ chain for several values of the plaquette threading flux). The eigenvalues for an arbitrary value of flux are given by

$$\epsilon_{\text{flat}} = 0, \quad \epsilon_{\pm} = \pm 2t \sqrt{1 + \cos(\phi/2) \cos(\phi'/N_c + k)}, \quad (4)$$

where k is the momentum.

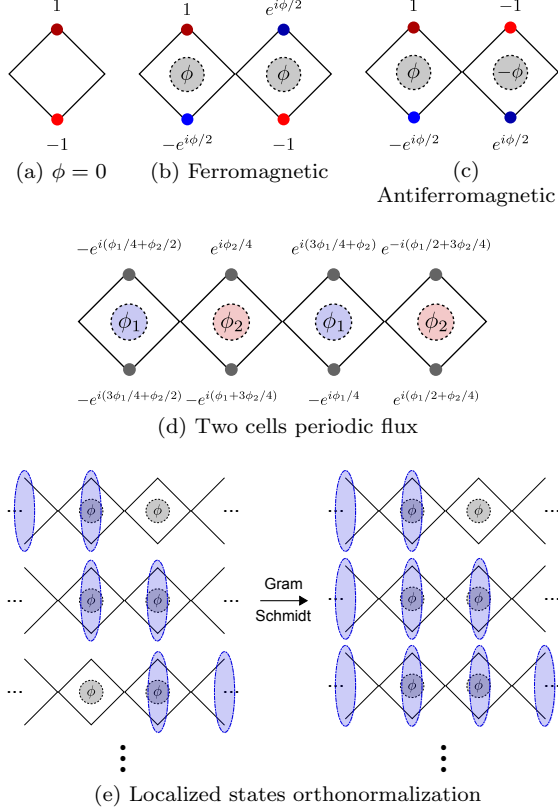


FIG. 4: (a), (b) and (c): Localized states for AB_2 chains without flux and threaded by ferromagnetic or anti-ferromagnetic flux, respectively. For simplicity the states are not normalized and we only draw the cells where the wavefunction is non-zero. (d) Localized states for $N = 2$, where N is the periodicity in the flux (in terms of number of cells). (e) Our non-orthonormal basis of localized states, occupying two cells, can be transformed into an orthonormal basis where they occupy, $1, 2, \dots, N_c$ cells, via the Gram-Schmidt procedure.

B. Localized states

Localized states associated with the flat band can be written in the most compact form as standing waves in one (in the absence of magnetic flux) or two consecutive plaquettes (in the presence of magnetic flux).²⁷ In the particular case of zero flux, localized states are simply the anti-bonding combination of the B and C states, $BC_j^- = (|B_j\rangle - |C_j\rangle)/\sqrt{2}$, and itinerant states in the AB_2 ring are linear combinations of A and bonding BC^+ states, $BC_j^+ = (|B_j\rangle + |C_j\rangle)/\sqrt{2}$. Rewriting the Hamiltonian in the basis of antibonding BC^- , bonding BC^+ and A states, one obtains a tight-binding ring of sites A and bonding BC sites (with hopping constant $\sqrt{2}t$) and a ring of decoupled anti-bonding BC states,²⁷ as shown in Fig. 2a.

The number of localized states is equal to the number of rhombi and in the presence of flux, if written in the most compact form (each localized state taking place in

two consecutive plaquettes) they form a non-orthogonal set of states. Orthogonalization of these set of states implies that the extension of the localized states ranges from two consecutive plaquettes to the complete ring (see Fig. 4e), except for $\phi = 0$ and for $\phi = \pi$ (in this case, the orthogonal localized states occupy only two consecutive plaquettes). This will imply a clear difference in the conductance when compared with the zero flux case. Note that a gap opens between the localized band and the itinerant bands when flux is present.

Assuming $\phi' = 0$ to simplify, the non-orthogonal localized states are of the form $(|B_j\rangle - e^{i\frac{\phi}{2}}|C_j\rangle) + (e^{i\frac{\phi}{2}}|B_{j+1}\rangle - |C_{j+1}\rangle)$ where the sites have been numbered clockwise in the AB_2 ring, that is, j indexes the plaquettes in the AB_2 ring.

Since the localized states have nodes at the A sites, we can write these localized states indicating only the one-particle state amplitudes at the pairs of B and C sites of the AB_2 ring, that is, we can write the localized state as a list with $2N_c$ entries $(b_1, c_1, \dots, b_n, c_n)$, where b_j and c_j are, respectively, the value of the wavefunction on site B_j and C_j . Then our localized states are,

$$|\psi_j\rangle = \frac{1}{\sqrt{4}} \left(0, \dots, 0, \underbrace{1}_{b_j}, \underbrace{-e^{-i\phi/2}}_{c_j}, \underbrace{e^{-i\phi/2}}_{b_{j+1}}, \underbrace{-1}_{c_{j+1}}, 0, \dots, 0 \right) \quad (5)$$

Note that for $\phi = 0$, we have for $|\psi_j\rangle$ that $b_j = b_{j+1}$ and $c_j = c_{j+1}$, and for $\phi = \pi$, $\langle\psi_j|\psi_{j+1}\rangle = 0$. There are many possible ways of constructing an orthogonal basis for the subspace of localized states. Our results for the conductance are obviously independent of this choice. We simply use the Gram-Schmidt orthogonalization, starting with the basis

$$\begin{aligned} |\psi_1\rangle &= \frac{1}{\sqrt{4}} (1, -e^{-i\phi/2}, e^{-i\phi/2}, -1, 0, \dots, 0), \\ |\psi_2\rangle &= \frac{1}{\sqrt{4}} (0, 1, -e^{-i\phi/2}, e^{-i\phi/2}, -1, 0, \dots, 0), \\ &\vdots \\ |\psi_{N_c}\rangle &= \frac{1}{\sqrt{4}} (e^{-i\phi/2}, -1, 0, \dots, 0, 1, -e^{-i\phi/2}). \end{aligned} \quad (6)$$

For such a basis we have

$$\langle\psi_i|\psi_j\rangle = \delta_{i,j} + \frac{\cos\phi/2}{2} (\delta_{i-1,j} + \delta_{i+1,j}). \quad (7)$$

For simplicity, let us define the support of a wavefunction, denoted by supp , to be those site where the wavefunction is non-zero. Then we have $\text{supp} |\psi_j\rangle = \{B_j, C_j, B_{j+1}, C_{j+1}\}$.

Let $\{|\phi_j\rangle\}_{j=1}^{N_c}$ denote the orthonormalized basis after the G-S procedure, defined by the recursive expression,

$$\begin{aligned}
|\phi'_j\rangle &= |\psi_j\rangle - \sum_{i=1}^{j-1} \langle\phi_i|\psi_j\rangle |\phi_i\rangle, \\
|\phi_j\rangle &= \frac{|\phi'_j\rangle}{\sqrt{\langle\phi'_j|\phi'_j\rangle}}.
\end{aligned} \tag{8}$$

We focus on $\phi \neq \pi$ (for in that case, the basis is already orthonormalized) and begin by making $|\phi_1\rangle = |\psi_1\rangle$, which implies $\text{supp } \phi_1 = \{B_1, C_1, B_2, C_2\}$. Then $|\phi'_2\rangle = |\psi_2\rangle - \langle\phi_1|\psi_2\rangle |\phi_1\rangle$. In this case, since $\langle\phi_1|\psi_2\rangle \neq 0$, $\text{supp } \phi_2 = \{B_1, C_1, B_2, C_2, B_3, C_3\}$. We then have $|\phi'_3\rangle = |\psi_3\rangle - \langle\phi_2|\psi_3\rangle |\phi_2\rangle - \langle\phi_1|\psi_3\rangle |\phi_1\rangle$. Note that $|\phi_1\rangle$ and $|\psi_3\rangle$ have disjoint support, hence $\langle\phi_1|\psi_3\rangle = 0$. Also, $\langle\phi_2|\psi_3\rangle \propto \langle\psi_2|\psi_3\rangle \neq 0$. Since $\text{supp } |\psi_3\rangle = \{B_3, C_3, B_4, C_4\}$ and $\text{supp } \phi_2 = \{B_1, C_1, \dots, B_3, C_3\}$, and since, there is no destructive interference on sites B_3 and C_3 (it is a simple exercise to show this), $\text{supp } \phi_3 = \{B_1, C_1, \dots, B_4, C_4\}$. Continuing the above procedure we finally arrive at

$$\text{supp } |\phi_j\rangle = \{B_1, C_1, \dots, B_{j+1}, C_{j+1}\}. \tag{9}$$

and therefore the extension of the orthogonalized localized states (constructed this way) ranges between two consecutive plaquettes and the full AB_2 ring. This is illustrated schematically in Fig. 4e.

However, as we have already mentioned, one has two exceptions:

i) for $\phi = 0$, the states $|\alpha_j\rangle = (0, \dots, 0, \underbrace{1}_{b_j}, \underbrace{-1}_{c_j}, 0, \dots, 0)$ already constitute an

orthogonal set of localized states for $\phi = 0$ as stated in the previous paragraph;

ii) for $\phi = \pi$, $\langle\psi_j|\psi_{j+1}\rangle = 0$ are orthogonal and in this case the range of the localized states in their most compact form is just two plaquettes.

There are many possible ways of constructing an orthogonal basis for the subspace of localized states. It must be stressed that our results for the conductance are obviously independent of this choice.

Using the construction for localized states of²⁷, it is easy to extend some of the results presented in this paper to geometries other than the AB_2 geometry. To make this more concrete let us give some examples. Let us start by considering an AB_2 chain with an arbitrary number of cells. Assume, for now, that the flux through each cell has the same value, a situation we call *ferromagnetic* (shown in Fig. 4b). Then, localized states occupying only two cells can be found for an arbitrary value of flux (albeit non orthogonal, except when $\phi = \pi$),²⁷ while for zero flux one can find localized states occupying only one cell as shown in Fig. 4a. Now consider a situation where the magnetic flux through each plaquette is symmetric to the one threading its neighboring cells, a situation we call *anti-ferromagnetic*. Then a similar state to the situation above can be found as is shown in Fig. 4c. For

this particular case, using this construction, we can find localized states that occupy two cells. However, these states form an orthonormal basis only for $\phi = \pi$ and for the ferromagnetic flux situation, as can be readily seen calculating the overlap between neighboring states. Let $|\psi_j\rangle$ be the state localized in the j th and $(j+1)$ th cells. For the ferromagnetic situation the overlap between neighboring states is $\langle\psi_{j+1}|\psi_j\rangle = \frac{\cos(\phi/2)}{2}$ while for the

anti-ferromagnetic situation one has $\langle\psi_{j+1}|\psi_j\rangle = -\frac{1}{2}$. Note that this flux threading each cell is not necessarily an external flux, since it may be generated by the spin of an atom/molecule, embedded into the chain as is the case of some copper oxide systems, namely CuO_4 chains^{28,29}.

If the flux through each plaquette is distinct, but repeats every N cells (Fig. 4d shows the situation for $N = 2$), one can also use the same construction to find localized states. In this case however, one must consider $2N$ adjacent cells instead of 2, as before, and we will find a localized states that extend through $2N$ cells. As before, these are not necessarily orthonormal, but can be made so by using Gram-Schmidt orthonormalization. In the extreme case, where there is no periodicity, translational invariance is obviously broken and our procedure will give us an extended state instead. A particular case of the $N = 2$ situation, with $\phi_1 = 2\phi_2$ has been studied in³⁰.

III. CONDUCTANCE THROUGH THE AB_2 RING

In this section we discuss the conductance through the AB_2 ring. We will begin by addressing the case without magnetic flux. Since no two-particle interactions are considered in this paper, the transmission probability $|t(\omega)|^2$ for an incident particle with momentum k and energy $\omega = -2\cos(k)$ can be calculated using quantum scattering theory³¹, and is given by the following expression³²,

$$\begin{aligned}
|t(\omega)|^2 &= 4t_L^2 t_R^2 \sin^2 k |\langle R | [\epsilon_k \hat{I}_s - H_s \\
&\quad + e^{ik} (t_L^2 |L\rangle \langle L| + t_R^2 |R\rangle \langle R|)]^{-1} |L\rangle|^2, \tag{10}
\end{aligned}$$

where the inverse is to be found within the subspace of the cluster sites (in our case, the AB_2 ring) positions and \hat{I}_s is the identity operator in that subspace. This equation includes the effect of the coupling of the ring to the leads as modifications of the on-site energies of sites L and R . If the conductance is normalized by the conductance of an ideal one dimensional system, $G_0 = e^2/\pi\hbar$, then the conductance is given by the transmission probability at the chemical potential.³³ In what follows, we will always deal with this normalized conductance, i.e., transmission probability.

In Fig. 5, we show several profiles of the conductance through the AB_2 ring with four unit cells as function of the energy of the incident electron (or chemical potential of the leads) or as function of a potential V_{gate} applied

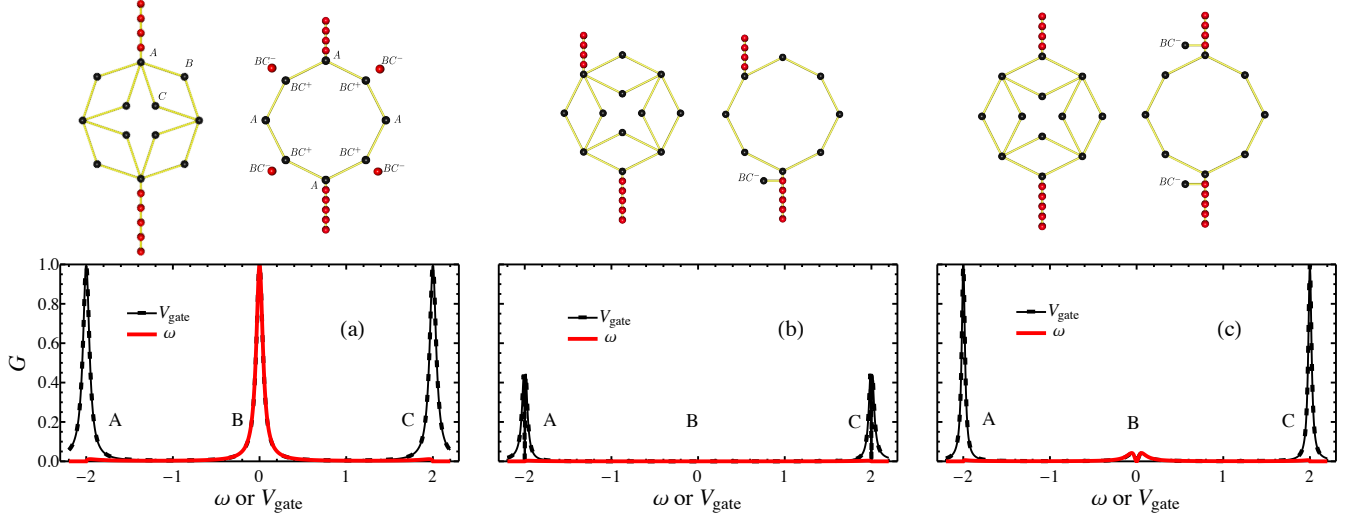


FIG. 5: Normalized conductance through the AB_2 ring as function of the energy of the incident electron (or chemical potential of the leads) and as function of V_{gate} for several positions of the leads. The positions of the leads are shown on the top figures. We show beside the AB_2 circuits, figures of equivalent systems which have exactly the same conductance profiles. Parameters: $t_L = t_R = 0.3t$.

to the AB_2 ring. These profiles correspond to certain positions of the leads which are shown at the top of the Fig. 5a, Fig. 5b and Fig. 5c. In these figures we also include diagrams of equivalent systems, that is, systems that exhibit exactly the same conductance profiles as the AB_2 ring.

In the case of Fig. 5a, the leads are connected to sites A, therefore the anti-bonding BC "sites" can be ignored since they are completely decoupled from the leads. The remaining "ring" of sites A and bonding BC sites form a tight binding ring. Therefore, if the contacts are sites A, the conductance is exactly the same as that of the equivalent tight-binding ring (with hopping constant $\sqrt{2}t$).³⁴ For small coupling between the leads and the AB_2 ring, the conductance has peaks when the chemical potential coincides with any of the system eigenvalues of the AB_2 ring, due to resonant tunnelling. These peaks have the Breit-Wigner shape. In Fig. 5a, three peaks A, B and C are observed in $G(V_{\text{gate}})$ in a potential interval corresponding to the bandwidth of the leads (the chemical potential of the leads is equal to zero). The same peaks should also be observed in the $G(\omega)$ -plot of Fig. 5a where $V_{\text{gate}} = 0$ and the chemical potential (or equivalently the energy ω of the incident particle) is varied from the bottom of the leads band to the top. However peaks A and B are absent because they correspond to the bottom and top energies of the leads bands and the particle velocity is zero for these energies.

If the left contact is a site B or C (let us assume it is a site B) and the right contact is a site A, as in the case of Fig. 5(b), the conductance profile is the same as that of a tight-binding ring but with the $\omega = 0$ peak absent. This absence reflects the fact that the hopping term from the left lead to a B site of the AB_2 ring, in the basis of

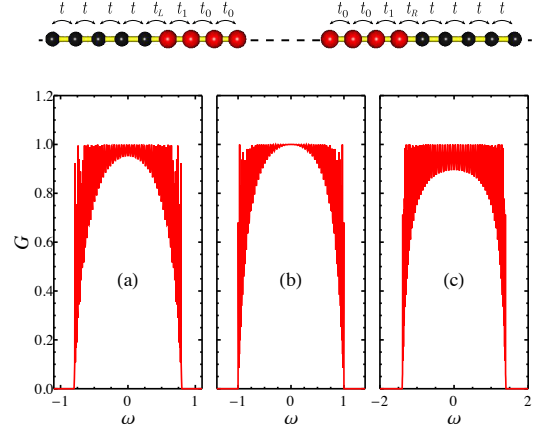


FIG. 6: The conductance through the AB_2 ring (or a linear ring) in the absence of flux and with opposite contacts at sites A is the same as for a linear chain (shown in the top figure, where the larger, red sites replace the AB_2 ring). In (b), one has the conductance for the particular case of $2t_1/\sqrt{2} = 2t_0 = t_L = t_R = 1$ in units of t and one sees that the central cluster (corresponding to the AB_2 ring) becomes transparent to an incoming particle for energies around zero, i.e., the bond with hopping constant t_1 acts as a monoatomic anti-reflection coating between the regions with hoppings t and t_0 . Deviations of the hopping constants from the previous values introduce oscillations in the conductance for energies around zero, as shown in (a) and (c) (where $t_1/\sqrt{2} = t_0 = .4$ and $t_1/\sqrt{2} = t_0 = .7$, respectively).

antibonding BC^- , bonding BC^+ and A states, becomes a hopping between the left lead and a bonding state bonding BC^+ and a hopping to a localized state BC^- , both with a smaller hopping constant $t_L/\sqrt{2}$. Since this localized state is decoupled from all other states of the ring, it only leads to a reflected wave back into the left lead. For $\omega = 0$, this reflected wave interferes destructively with the incident wave and one can say the localized state BC^- acts as a conductance absorber for frequencies close to $\omega = 0$ (in close analogy with $\lambda/4$ sound absorbers). The absence of the $\omega = 0$ peak can also be explained in the following way. The hopping to the BC^- "site" is a "dangling bond". If one considers a linear chain with a dangling site as shown in Fig. 2c (with hopping constant t_a to the dangling site), then the equation for the wavefunction amplitude ψ_a at the dangling site of a particle with energy $\omega = -2t \cos(k)$ is $\omega \psi_a = -t_a \psi_j$. Substituting ψ_a in the equation for the wavefunction amplitude at site j , ψ_j , one has $\omega \psi_j = -t \psi_{j-1} - t \psi_{j+1} + (t_a^2/\omega) \psi_j$, therefore the dangling site effectively modifies the on-site energy of site j to $\epsilon_j(\omega) = (t_a^2/\omega)$. When $\omega = 0$, the on-site energy becomes infinite and one has zero conductance at $\omega = 0$. The peaks A and C in Fig. 5(b) have a reduced amplitude compared to those in Fig. 5a due to the difference in paths in the upper and lower arms of the ring.

If both the left and right contacts are sites B (or C) as shown in Fig. 5(c), an analogous reasoning applies and the system is equivalent to a linear ring connected to leads but with two dangling sites, one at the end of each lead. Again, localized states act as a filter of the $\omega = 0$ peak.

In the case of Fig. 5a, the remaining "ring" of sites A and bonding BC sites can be mapped onto a linear chain since the leads are coupled to opposite A sites. In this case, the leads define an axis of symmetry of the diamond ring and the anti-bonding combinations of an A (or bonding BC) site with the one obtained by reflection in this axis of symmetry are decoupled from the contact sites, or equivalently, the tight-binding hoppings from the contact sites generate a bonding combination of the nearest-neighbor bonding BC "sites" and this bonding combination couples only to the bonding combination of A sites. So, for the purpose of calculating the conductance across the AB_2 ring, it is enough to consider the linear sequence of these bonding states (see the top diagram in Fig. 6 where the cluster of larger, red sites replaces the AB_2 ring). In Fig. 6b, one has the conductance for the particular case of $2t_1/\sqrt{2} = 2t_0 = t_L = t_R = 1$ in units of t , that is, we have three regions with different hopping constants t , t_0 and t , separated by single hoppings of constant t_1 . The central cluster (and therefore also the AB_2 ring) becomes transparent to the incoming particle for energies around zero. Deviations of the hopping constants from the previous values introduce oscillations in the conductance for energies around zero, as shown in Fig. 6a and Fig. 6c, where the dome of minima of the conductance oscillations is below one.

This result can be explained with an analogy with a quarter wavelength anti-reflection coating³⁵, that is, the bond with hopping constant t_1 acts as a monoatomic anti-reflection coating between the regions with hopping constant t and t_0 . A anti-reflection coating generates an additional reflected wave which is out of phase with the first reflected wave and therefore partially cancels the reflection. If the refraction index of the coating is the geometric mean of the refraction indices of the materials to the left and right of the coating, $n_c = \sqrt{n_{\text{left}} n_{\text{right}}}$, the transmittance becomes one when the wavelength of incident wave, λ , is such that the thickness of the coating is an odd multiple of the $\lambda/4$. This can be translated into our problem in the following way. The relation $n_c = \sqrt{n_{\text{left}} n_{\text{right}}}$ can be written as $n_c/n_{\text{right}} = \sqrt{n_{\text{left}}/n_{\text{right}}}$ which is equivalent to a relation between velocities $v_{\text{right}}/v_c = \sqrt{v_{\text{right}}/v_{\text{left}}}$. The ratio between velocities in our system for energies close to zero is approximately the ratio of hopping constants and the previous relation becomes $t_1/t_0 = \sqrt{t/t_0}$. So perfect transmission occurs when $2t_1/\sqrt{2} = 2t_0 = t$ (as in the case of Fig. 6b) and when $\lambda/4$ is equal to one interatomic distance (which we have assumed to be one), that is, for $k = \pi/2$ or equivalently, energy $\omega = -2t \cos(k)$ equal to zero.

When magnetic flux is present, a gap opens between the flat band and the itinerant bands of the AB_2 ring. The conductance peaks corresponding to energies of itinerant states follow the behavior of the conductance peaks of a linear ring and we do not address them here (see³⁴). The behavior of the conductance for energies close to $\omega = 0$ (which is determined only by the localized states of the AB_2 ring when flux is finite and the coupling between the leads and the cluster is small) is rather unusual. A zero frequency dipped conductance peak is observed despite the fact that the energies of the itinerant states of the ring are far from this zero frequency peak. This is shown in Fig. 7a for the case of an AB_2 ring with 16 unit cells and for $\phi = \pi/2$. This dipped peak only occurs if the contact sites are sites B or C (otherwise the peak is absent) and shows distinct behavior as function of the positions of the contact sites and as function of the magnetic flux. As shown in the inset of Fig. 7a, the peak maximum decays quasi-exponentially as a function of the contact sites distance, except for the first two distances, where the conductance peak maximum remains the same. Such behavior is also visible in Fig. 8 where the logarithm of the conductance for small frequencies of an incident particle is plotted for several inequivalent positions of the leads. The dependence with flux of the maximum of the conductance peak shows rather peculiar behavior depending on the position of the contacts. In Fig. 7b, we show the maximum of the $\omega = 0$ conductance peak as a function of the flux threading each plaquette, ϕ , for several choices of contacts positions. When the contacts are the sites B_1 and C_1 (see the labeling of the sites in the inset of Fig. 7a), the maximum starts at one, oscillates for small ϕ and goes smoothly to zero as ϕ

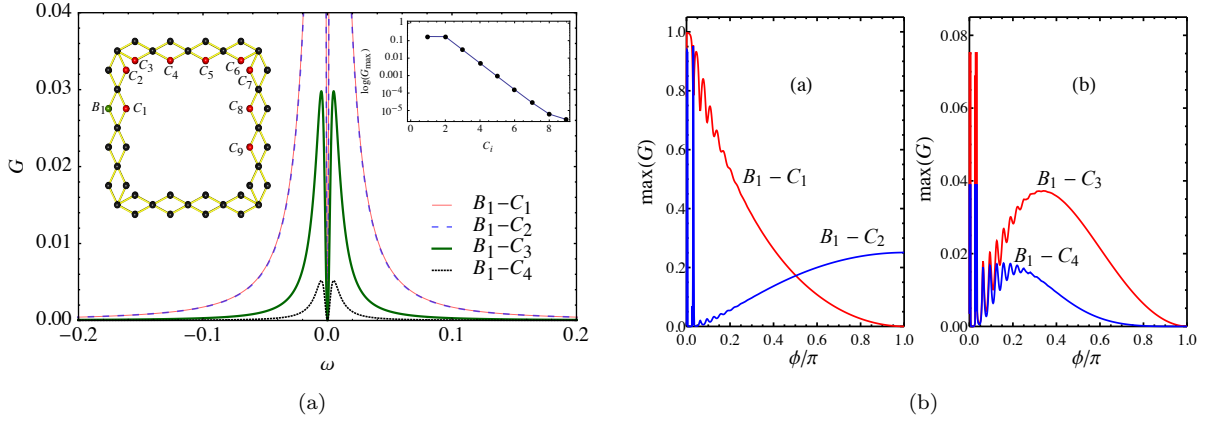


FIG. 7: (a) Conductance as a function of the frequency of the incident particle for an AB_2 ring of 16 plaquettes, $\phi = \pi/2$, and several positions of the leads contacts. For this flux value, only localized states contribute significantly to the $\omega = 0$ conductance peak. (b) Maximum of the conductance as a function of the flux for 16 plaquettes. For leads contacts at B_1-C_2 and $\phi = \pi$, the peak value of the conductance is 0.25, since in this case the AB_2 is mapped onto the cluster of Fig. 9a with equal values of the hopping constants. For leads at B_1-C_1 it is zero for $\phi = \pi$, since the left and right leads couple to orthogonal states which do not overlap. The oscillations at low flux reflect dependence of the inner magnetic flux ϕ_i and disappear as the gap between the itinerant bands and the localized states grows with increasing flux.

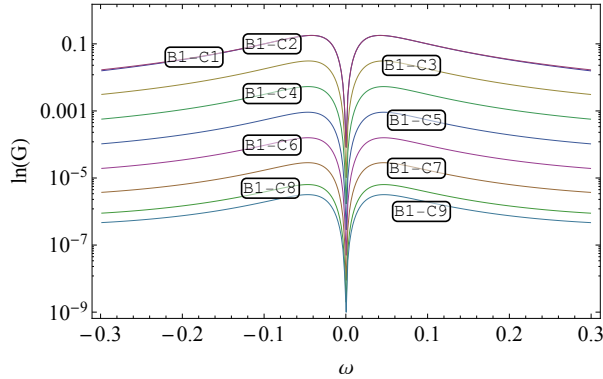


FIG. 8: Logarithm of the conductance for 16 cells and $\phi = \pi/2$ around $\omega = 0$, for all the inequivalent lead positions such that one of the leads is on a B site and the other on a C site.

approaches π . The oscillations near $\phi = 0$ reflect the contribution to the conductance of the itinerant states which oscillates as a consequence of the Aharonov-Bohm effect due to the varying flux threading the inner region of the AB_2 ring (an uniform field was applied to the AB_2 cluster). These oscillations disappear as ϕ grows due to the larger gap between the itinerant bands and the $\omega = 0$ energy. Note that localized states do not “feel” this inner flux, that is, their energy is independent of this field and therefore do not contribute to an Aharonov-Bohm effect. When the contacts are the sites B_1 and C_2 , contrasting behavior occurs and the maximum approaches zero when ϕ is small and tends to 0.25 when ϕ goes to π . For larger distance between contacts, the graphs of the maximum of the $\omega = 0$ conductance peak exhibit dome-like profiles (see Fig. 7b(b)), with the peak maximum growing from

near zero when ϕ is small, reaching a maximum value and decreasing to zero when ϕ approaches π .

These results can be explained recalling our previous discussion of the extension of localized states when the flux is finite. Since this extension ranges from two unit cells to the full ring, and ignoring the itinerant states of the ring which are energetically far from the $\omega = 0$ energy region, the conductance is only finite if one has localized states that extend from the left contact to the right contact in the AB_2 ring. More precisely, we can divide the localized states in the following way: states I that extend from the left contact to the right contact, that is, that have finite wavefunction amplitudes at the sites L and R of the AB_2 ring; states II that have finite wavefunction amplitudes at the site L but not at the site R of the AB_2 ring; states III that have finite wavefunction amplitudes at the site R but not at the site L of the AB_2 ring; states IV that have zero wavefunction amplitudes at both the sites L and R of the AB_2 ring. Note that the choice of basis for the subspace of localized states influences the number of states in each of these groups, but the explanation for the conductance results remains the same. The larger the extension of the localized states, the smaller the wavefunction amplitude at the contact sites, and consequently the smaller the effective hopping between the extremities of the leads and the localized state. So, our system is equivalent to that displayed in the top diagram of Fig. 9a. The hopping constants between the leads (smaller, red spheres) and the localized states (larger, black spheres) are in general different but all these hopping can be simplified and the system can be reduced to that shown in the bottom diagram of Fig. 9a. In fact, several dangling sites (states II) contribute to the on-site energy of the site at the end of the left lead and

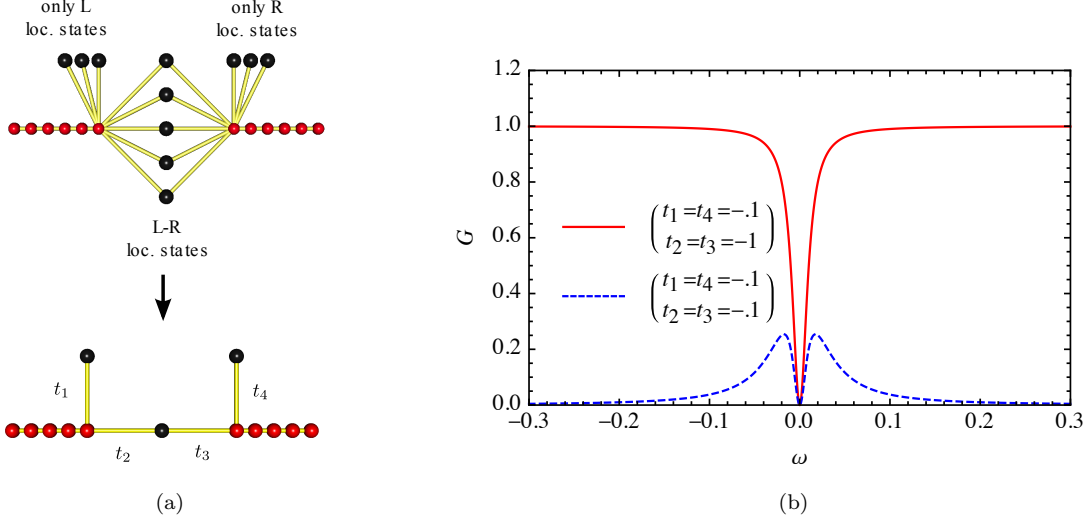


FIG. 9: (a) The coupling of the leads to the localized states of the AB_2 ring in the presence of flux is described by the top diagram where one has dangling sites connected to the left (right) lead representing the localized states which have finite wavefunction amplitude at site L (R), but zero amplitude at site R (L). The system on top is equivalent to the bottom system consisting of only one L, R and LR localized states. (b) Whenever all hopping constants in the bottom system are equal, the maximum of the conductance is 0.25 regardless of their value. Due to the dangling sites, the conductance always goes to zero at zero frequency.

t_1 is the hopping constant that generates an on-site energy equal to the sum of the on-site energies generated by the dangling sites at the left lead. The same goes for t_4 . The effect of the localized states of the type I can also be reproduced with a single site but with different hopping constants to the left lead and to the right lead. In Fig. 9b, we show the conductance through this simplified system. If $t_2 = t_4 = t$, without the dangling sites, we would have perfect transmittance for any energy of the incident electron. The effect of the dangling sites is the creation of the dip at $\omega = 0$ as one can see in Fig. 9b (red solid curve). If t_2 and t_3 are rather smaller than t and no dangling site is present ($t_1 = t_4 = 0$), a peak appears at $\omega = 0$ of width proportional to t_2 (assuming $t_2 = t_3$). The effect of the dangling sites in this case is again the introduction of the dip at the center of this peak. If the width of the dip becomes larger than that of the peak, the dipped peak maximum becomes small.

One can now explain the behavior displayed in Fig. 7b. One should recall that the non-orthogonal localized states are of the form

$(|B_j\rangle - e^{i\frac{\phi}{2}}|C_j\rangle) + (e^{i\frac{\phi}{2}}|B_{j+1}\rangle - |C_{j+1}\rangle)$. The overlap between consecutive localized states is equal to $\cos(\phi/2)/2$, so it is zero whenever $\phi = \pi$, and $1/2$ when $\phi = 0$ (the latter value implies that shorter and orthogonal localized states can be found of the form $BC_j^- = 1/\sqrt{2}(|B_j\rangle - |C_j\rangle)$). We consider only the mean evolution of the conductance, that is, the dependence of the conductance remaining if the oscillations due to the Aharonov-Bohm effect are removed. This behavior consists of the following: if the contacts are the sites B_1 and C_1 , the maximum of the conductance

is one for zero flux and with increasing magnetic flux, the conductance decreases and becomes zero for flux equal to π . Note that for $\phi = \pi$, the localized states, $|\psi_j\rangle = 1/2(|B_j\rangle - i|C_j\rangle) + (i|B_{j+1}\rangle - |C_{j+1}\rangle)$, are orthogonal and both leads couple to only two of these states, $|\psi_1\rangle$ and $|\psi_{N_c}\rangle$. That is, we have only two states of type I and all other localized states are of type IV. The transport through the cluster is given by the transfer terms to these localized states of the form $\langle\psi_1|H|0\rangle$ which collected (omitting the hopping terms in the leads) give rise to $(-t_L/2)|0\rangle[\langle\psi_1|+i\langle\psi_{N_c}|] + (-t_R/2)|N+1\rangle[-i\langle\psi_1| - \langle\psi_{N_c}|] + \text{H.c.}$ But $[\langle\psi_1|+i\langle\psi_{N_c}|]$ and $[-i\langle\psi_1| - \langle\psi_{N_c}|]$ are orthogonal bras, therefore the left and right leads are effectively decoupled and the transmittance is zero. A similar reasoning can be followed when ϕ approaches zero. In this case the leads couple to only one localized state, $BC_1^- = 1/\sqrt{2}(|B_1\rangle - |C_1\rangle)$, that is, we have one state of type I and no dangling sites, so the transmittance approaches one.

If the contacts are the sites B_1 and C_2 , the maximum of the conductance is zero for zero flux and, with increasing magnetic flux, the conductance increases and becomes $1/4$ for flux equal to π . The fact that the conductance maximum approaches zero as ϕ goes to zero is common to all other contact possibilities with exception of the previous one and reflects a similar argument, that is, the left lead couples to only one localized state, $BC_1^- = 1/\sqrt{2}(|B_1\rangle - |C_1\rangle)$ and the right lead couples only to one other localized state which is orthogonal to the former, and consequently the transmittance is zero. The fact the conductance goes to $1/4$ when the flux goes to π can also be justified as before, collecting the trans-

fer integrals and one has $(-t_L/2)|0\rangle[\langle\psi_1| + i\langle\psi_{N_c}|] + (-t_R/2)|N+1\rangle[-\langle\psi_1| - i\langle\psi_2|] + \text{H.c.}$, and this corresponds to the bottom diagram displayed in Fig. 9b with $t_1 = it_L/2$, $t_4 = -it_L/2$, $t_2 = t_L/2$, and $t_3 = t_R/2$. Since we considered $t_L = t_R$, all these hopping constants are equal in absolute value and therefore the conductance is equal to 1/4 in agreement with what is shown in Fig. 9b. Note that the phase terms are irrelevant at the dangling sites.

If one of the contacts is the site B_1 and the other is a C_j site with $j \neq N_c, 1, 2$, the maximum of the conductance goes to zero as the flux goes to zero and with increasing magnetic flux, the conductance increases, reaches a maximum (this maximum becomes smaller as the distance between contacts increases) and goes again to zero when the flux approaches π , reflecting the fact that the orthogonal localized states are all two unit cells long.

IV. CONCLUSIONS

We have shown that localized states in itinerant geometrically frustrated electronic systems generate rather striking behavior in the two terminal electronic conductance. In the absence of magnetic flux, the localized states act as a filter of the zero frequency conductance peak (we suggested an analogy with $\lambda/4$ sound absorbers), if there is a finite hopping probability between the leads contact sites and the localized states. In contrast, when magnetic flux is present, some localized states contribute to the appearance of a zero frequency conductance peak while other localized states act as a

conductance absorber, and as a consequence, the conductance exhibits a zero frequency peak with a dip.

We have shown that such different roles of the localized states are due to the fact that the presence of magnetic flux implies that any orthogonal basis of the subspace of localized states is composed of localized states with variable extensions (ranging from two unit cells to the complete ring, in the case of the AB_2 ring studied in this paper). Such peculiar dipped peak fixed at the localized states energy, even when magnetic flux is varied, is a distinct fingerprint of the existence of localized states in itinerant geometrically frustrated electronic systems. Furthermore, depending on the distance between contact sites, different profiles for the maximum of the dipped conductance peak as function of the magnetic flux have been obtained, and this implies that the two terminal conductance can be used as a probe of the localized states spatial dependence.

Acknowledgements

A. A. Lopes acknowledges the financial support of the Portuguese Science and Technology Foundation (FCT), cofinanced by FSE/POPH, under grant SFRH/BD/68867/2010 and of the Excellence Initiative of the German Federal and State Governments (grant ZUK 43). R. G. Dias acknowledges the financial support from the Portuguese Science and Technology Foundation (FCT) through the program PEst-C/CTM/LA0025/2013.

-
- ¹ C. Gorter, *Physica* **17**, 777 (1951), ISSN 0031-8914, URL <http://www.sciencedirect.com/science/article/pii/0031891451900985>.
 - ² B. J. van Wees, H. van Houten, C. W. J. Beenakker, J. G. Williamson, L. P. Kouwenhoven, D. van der Marel, and C. T. Foxon, *Phys. Rev. Lett.* **60**, 848 (1988), URL <http://link.aps.org/doi/10.1103/PhysRevLett.60.848>.
 - ³ A. D. Stone and P. A. Lee, *Phys. Rev. Lett.* **54**, 1196 (1985), URL <http://link.aps.org/doi/10.1103/PhysRevLett.54.1196>.
 - ⁴ Y. Aharonov and D. Bohm, *Phys. Rev.* **115**, 485 (1959), URL <http://link.aps.org/doi/10.1103/PhysRev.115.485>.
 - ⁵ R. A. Webb, S. Washburn, C. P. Umbach, and R. B. Laibowitz, *Phys. Rev. Lett.* **54**, 2696 (1985), URL <http://link.aps.org/doi/10.1103/PhysRevLett.54.2696>.
 - ⁶ Z. Gulacsi, A. Kampf, and D. Vollhardt, *Phys. Rev. Lett.* **99**, 026404 (2007), URL <http://link.aps.org/doi/10.1103/PhysRevLett.99.026404>.
 - ⁷ H. Kikuchi, Y. Fujii, M. Chiba, S. Mitsudo, T. Idehara, T. Tonegawa, K. Okamoto, T. Sakai, T. Kuwai, and H. Ohta, *Phys. Rev. Lett.* **94**, 227201 (2005), URL <http://link.aps.org/doi/10.1103/PhysRevLett.94.227201>.
 - ⁸ A. M. S. Macedo, M. C. dos Santos, M. D. Coutinho-

- Filho, and C. A. Macedo, *Phys. Rev. Lett.* **74**, 1851 (1995), URL <http://link.aps.org/doi/10.1103/PhysRevLett.74.1851>.
- ⁹ R. R. Montenegro-Filho and M. D. Coutinho-Filho, *Phys. Rev. B* **74**, 125117 (2006), URL <http://link.aps.org/doi/10.1103/PhysRevB.74.125117>.
- ¹⁰ J. Vidal, R. Mosseri, and B. Doucot, *Phys. Rev. Lett.* **81**, 5888 (1998), URL <http://link.aps.org/doi/10.1103/PhysRevLett.81.5888>.
- ¹¹ H. Tamura, K. Shiraishi, T. Kimura, and H. Takayanagi, *Phys. Rev. B* **65**, 085324 (2002), URL <http://link.aps.org/doi/10.1103/PhysRevB.65.085324>.
- ¹² H. Tasaki, *Prog. Theor. Phys.* **99**, 489 (1998), ISSN 0033-068X, 1347-4081, URL <http://ptp.oxfordjournals.org/content/99/4/489>.
- ¹³ A. Mielke, *Phys. Rev. Lett.* **82**, 4312 (1999), URL <http://link.aps.org/doi/10.1103/PhysRevLett.82.4312>.
- ¹⁴ O. Derzhko and J. Richter, *Phys. Rev. B* **72**, 094437 (2005), URL <http://link.aps.org/doi/10.1103/PhysRevB.72.094437>.
- ¹⁵ J. Richter, O. Derzhko, and J. Schulenburg, *Phys. Rev. Lett.* **93**, 107206 (2004), URL <http://link.aps.org/doi/10.1103/PhysRevLett.93.107206>.
- ¹⁶ O. Derzhko, J. Richter, A. Honecker, M. Maksymenko, and

- R. Moessner, Phys. Rev. B **81**, 014421 (2010), URL <http://link.aps.org/doi/10.1103/PhysRevB.81.014421>.
- ¹⁷ A. Tanaka and H. Tasaki, Phys. Rev. Lett. **98**, 116402 (2007), URL <http://link.aps.org/doi/10.1103/PhysRevLett.98.116402>.
- ¹⁸ Y. F. Duan and K. L. Yao, Phys. Rev. B **63**, 134434 (2001), URL <http://link.aps.org/doi/10.1103/PhysRevB.63.134434>.
- ¹⁹ Z. Gulacsi and D. Vollhardt, Phys. Rev. B **72**, 075130 (2005), URL <http://link.aps.org/doi/10.1103/PhysRevB.72.075130>.
- ²⁰ Z. Gulacsi and D. Vollhardt, Phys. Rev. Lett. **91**, 186401 (2003), URL <http://link.aps.org/doi/10.1103/PhysRevLett.91.186401>.
- ²¹ J. Richter, J. Schulenburg, A. Honecker, J. Schnack, and H.-J. Schmidt, J. Phys.: Condens. Matter **16**, S779 (2004), ISSN 0953-8984, URL <http://iopscience.iop.org/0953-8984/16/11/029>.
- ²² K. C. Rule, A. U. B. Wolter, S. Sullow, D. A. Tennant, A. Bruhl, S. Kohler, B. Wolf, M. Lang, and J. Schreuer, Phys. Rev. Lett. **100**, 117202 (2008), URL <http://link.aps.org/doi/10.1103/PhysRevLett.100.117202>.
- ²³ J. Schulenburg, A. Honecker, J. Schnack, J. Richter, and H.-J. Schmidt, Phys. Rev. Lett. **88**, 167207 (2002), URL <http://link.aps.org/doi/10.1103/PhysRevLett.88.167207>.
- ²⁴ C. Wu, D. Bergman, L. Balents, and S. Das Sarma, Phys. Rev. Lett. **99**, 070401 (2007), URL <http://link.aps.org/doi/10.1103/PhysRevLett.99.070401>.
- ²⁵ C. Wu and S. Das Sarma, Phys. Rev. B **77**, 235107 (2008), URL <http://link.aps.org/doi/10.1103/PhysRevB.77.235107>.
- ²⁶ M. E. Zhitomirsky and H. Tsunetsugu, Phys. Rev. B **75**, 224416 (2007), URL <http://link.aps.org/doi/10.1103/PhysRevB.75.224416>.
- ²⁷ A. A. Lopes and R. G. Dias, Phys. Rev. B **84**, 085124 (2011), URL <http://link.aps.org/doi/10.1103/PhysRevB.84.085124>.
- ²⁸ M. Matsuda, K. M. Kojima, Y. J. Uemura, J. L. Zarestky, K. Nakajima, K. Kakurai, T. Yokoo, S. M. Shapiro, and G. Shirane, Phys. Rev. B **57**, 11467 (1998), URL <http://link.aps.org/doi/10.1103/PhysRevB.57.11467>.
- ²⁹ J. Schlappa, K. Wohlfeld, K. J. Zhou, M. Mourigal, M. W. Haverkort, V. N. Strocov, L. Hozoi, C. Monney, S. Nishimoto, S. Singh, et al., Nature **485**, 82 (2012), ISSN 0028-0836, URL <http://www.nature.com/nature/journal/v485/n7396/full/nature10974.html>.
- ³⁰ J. L. Movilla and J. Planelles, Phys. Rev. B **84**, 195110 (2011), URL <http://link.aps.org/doi/10.1103/PhysRevB.84.195110>.
- ³¹ J. R. Taylor, *Scattering theory: the quantum theory of non-relativistic collisions* (Dover Publications, Mineola, NY, 2006), ISBN 0486450139 9780486450131.
- ³² T. Enss, V. Meden, S. Andergassen, X. Barnabe-Therault, W. Metzner, and K. Schonhammer, Phys. Rev. B **71**, 155401 (2005), URL <http://link.aps.org/doi/10.1103/PhysRevB.71.155401>.
- ³³ Y. Imry and R. Landauer, Rev. Mod. Phys. **71**, S306 (1999), URL <http://link.aps.org/doi/10.1103/RevModPhys.71.S306>.
- ³⁴ D. Kowal, U. Sivan, O. Entin-Wohlman, and Y. Imry, Phys. Rev. B **42**, 9009 (1990), URL <http://link.aps.org/doi/10.1103/PhysRevB.42.9009>.
- ³⁵ E. Hecht, *Optics* (Addison-Wesley, Reading, Mass., 2002), 4th ed., ISBN 0805385665 9780805385663 0321188780 9780321188786.